10-14 July 2016, Vienna, Austria

Continued Development of Compact Multi-gas Monitor for Life Support Systems Control in Space

Jesús Delgado-Alonso[*], Straun Phillips, David Berry, and Paul DiCarmine[†]
Intelligent Optical Systems, Inc. Torrance, CA, 90505

Cinda Chullen[‡]
NASA Lyndon B. Johnson Space Center, Houston, TX, 77058

and

Gregory Quinn[§]
Hamilton Sundstrand Space Systems International, Inc. A UTC Aerospace Systems Company, Windsor Locks, CT 06096

Miniature optical gas sensors based on luminescent materials have shown great potential as alternatives to NIR-based gas sensor systems for the Portable Life Support System (PLSS). The unique capability of luminescent sensors for carbon dioxide and oxygen monitoring under wet conditions has been reported, as has the fast recovery of humidity sensors after long periods of being wet. Lower volume and power requirements are also potential advantages over both traditional and advanced non-dispersive infrared (NDIR) gas sensors, which have so far shown longer life than luminescent sensors. In this paper we present the most recent results in the development and analytical validation of a compact multi-gas sensor unit based on luminescent sensors for the PLSS. Results of extensive testing are presented, including studies conducted in Intelligent Optical Systems laboratories, a United Technologies Corporation Aerospace Systems (UTC) laboratory, and a Johnson Space Center laboratory. The potential of this sensor technology for gas monitoring in PLSSs and other life support systems, and the advantages and limitations found through detailed sensor validation are discussed.

Nomenclature

EMI   = electromagnetic interference
EMU   = extravehicular mobility unit
EVA   = extravehicular activity
FOCS = fiber optic chemical sensor
ISS   = International Space Station
LED   = light emitting diode
ϕ = phase
NDIR = non-dispersive infrared
pCO_2 = partial pressure of carbon dioxide
PLSS = Portable Life Support System
pO_2 = partial pressure of oxygen
RH   = relative humidity
SBIR   = Small Business Innovation Research

[*] Senior Scientist, 2520 W. 237th Street, Torrance, CA 90505-5217.
[†] Analytical Chemist, 2520 W. 237th Street, Torrance, CA 90505-5217.
[‡] Project Engineer, Space Suit and Crew Survival Systems Branch, Crew and Thermal Systems Division, 2101 NASA Parkway/EC5.
[§] Staff Research Engineer, 1 Hamilton Rd, Windsor Locks, CT 06096-1000.

I. Introduction

ADVANCED space suit life support systems for the successful support of the International Space Station (ISS) and future human space exploration missions will require a new generation of carbon dioxide (CO_2) sensors capable of overcoming the limitations of current technology in excessively moist environments. Relative humidity in the ISS EMU typically ranges from 75% to 100% RH, so liquid condensation should be expected, and it has caused multiple sensor failures. Most existing gas sensors exhibit hysteresis after condensation, and poor accuracy near water vapor saturation. In addition to operating under moist conditions, top-level requirements for Extra Vehicular Activity (EVA) system improvements include reduction of system size, weight, and power, non-consumption of resources, increased hardware reliability, durability, and operating life. Environmental conditions include functionality in microgravity, low pressure, oxygen environments and, specifically in the PLSS, operation in moist gases. NASA requires space suit gas sensors that function reliably under these conditions and that minimize mass, volume, and power consumption.

Non-dispersive infrared (NDIR) sensing technology represents the current state-of-the-art for measuring CO_2 in the space suit, despite its limitations under wet conditions [1], because it has proven to meet most NASA requirements with good sensitivity, accuracy and stability. NDIR is a means of direct spectroscopy, measuring the absorption of the target gas, which is proportional to its concentration. Basically, an NDIR device incorporates a light source emitting light at a wavelength of maximum absorption of the target gas, a chamber, a photodetector, and an electronic module for system operation, control, and signal processing. The light is launched through a chamber where the gas to be analyzed is present, and the light intensity is detected by the photodetector. The absorption of light by the target gas reduces the intensity of the light detected, according to the Beer–Lambert law, and that attenuation is correlated with the gas concentration. Any light attenuation caused by any other effect and not by the target gas has to be avoided or compensated, and advanced techniques have been developed to do so [2]. However, avoiding the presence of liquid water in the chamber or compensating the system when that happens is a challenge, and sensor technologies for CO_2 that can operate at elevated humidity are sought by NASA [3].

An alternative to direct spectroscopy for gas monitoring is an indicator-based optical sensor [4]. This type of sensor monitors the optical properties of a gas permeable sensitive material, and they depend on the concentration of the target gas. Basically, the chamber of the NDIR sensors is replaced with the sensitive material. Still, a light source and a photodetector are used. Because the optical properties of the sensitive material are important but not those of the gas being analyzed, the presence of liquid water, particles, or dirt in the gas or on the top of the sensor element do not affect the light transmission.

In order to take advance of this, we have developed an indicator-based optical sensor for monitoring the main gas constituents in the PLSS, with the objective of overcoming the limitations of NDIR-based devices. In the sensor developed for the PLSS, the sensitive material is a luminescent indicator immobilized in a polymeric matrix. A specific indicator dye is selected for each of the target gases—oxygen, carbon dioxide and water vapor. The red emission of the sensitive materials is excited by means of a blue LED, and detected by either an avalanche photodiode or a photomultiplier. The luminescence of each specific indicator undergoes a measurable change with the concentration of the target gas. In the sensor we have developed, the time between absorption of the blue excitation light and emission of red luminescent is strongly affected by the concentration of the target gas. We have used phase-resolved luminescence detection to monitor that delay between the excitation and the emission [5], which enables us to produce low-power, compact multichannel units. In phase-resolved measurements, the excitation light is modulated into a sinusoidal waveform at a selected frequency; as a result, the luminescence from the sensitive material is modulated at the same frequency, and the instrument calculates the phase shift (or delay) between the excitation and the emission.

In a three year project, IOS has developed a compact phase-resolved luminescence detector incorporating four optical channels, and validated it for use as a readout unit for luminescent sensors for partial pressure of carbon dioxide, oxygen, and humidity [6]. We developed a compact gas flow-through cell incorporating the three luminescent sensors, and integrated the readout unit and sensor flow-through cell. A miniature optic gas sensor (MOGS) system for pCO_2, pO_2, pH_2O, and temperature was assembled and tested extensively in IOS laboratories under environmental conditions relevant to the PLSS, including varying temperature and humidity, water condensation, reduced pressure, nitrogen and oxygen background, and presence of chemical contaminants, and then two MOGS prototypes were tested extensively by UTC for analytical characterization. The results of the tests at UTC are presented here, and compared with the data collected previously at IOS.

II. Miniature Optical Gas Sensor Prototypes

The first version of the luminescence-based MOGS unit (MOGS v0.1, Figure 1) incorporates: (1) a phase-resolved luminescence detector or readout unit, (2) a sensor flow-through cell, incorporating the three gas sensor elements and an optical sensor for temperature, and (3) an optical cable. A laptop recorded the data. The unit was powered at 5 V, and communicated with the computer via a USB cable. The readout unit dimensions are 100 mm × 85 mm × 30 mm. Two types of sensor flow-through cells were assembled. Both cells were 55 mm × 15 mm × 10 mm, one incorporating 5 mm diameter sensor elements and the other 10 mm diameter sensor elements. The interface with the test rig was through two standard gas valves Swagelok SS-2P4T.
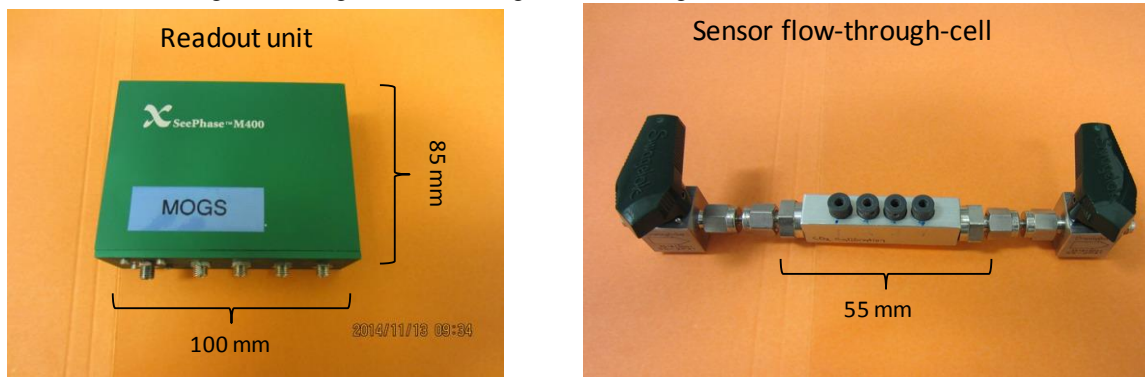
Figure 1. Components of the MOGS v0.1 unit incorporating manual valves to interface with the test rig.

III. Calibration Tests at IOS Laboratory

Two MOGS v0.1 prototypes were assembled, MOGS v0.1-5 mm and MOGS v0.1-10 mm, incorporating 5 mm diameter and 10 mm diameter sensor elements, respectively. The systems were calibrated in an IOS laboratory by exposing them to varied gas levels at varied humidity and temperature. The gas levels were controlled by means of mass flow controllers, and by mixing nitrogen with pure oxygen or pure carbon dioxide. The partial pressure of water and relative humidity was controlled by mixing gas saturated with water and dry gas, with mass flow controllers to control the flow rate of the moist and dry gas streams. In line with the MOGS system, we used a Horiba analyzer to monitor the CO_2 concentration, and a Vaisala probe to monitor the humidity.

The results of the calibration tests are a matrix of phase, gas level, and temperature for the oxygen and humidity sensors, and a matrix of phase, gas level, humidity, and temperature for the CO_2 sensor. With those matrixes we can calculate the gas level from the phase and temperature measurements. The complete calibration matrixes for all three sensors were calculated at eight temperature values from 4°C to 32°C; for the CO_2 sensors, four humidity levels from 20% RH to 95% RH were used at each of the eight temperatures. The CO_2 sensor was calibrated in the range from 0 to 15 mmHg pCO_2, the oxygen sensor was calibrated in the range from 0 to 450 mmHg pO_2, with particular detail in the 150 to 450 mmHg pO_2 range, and the humidity sensor was calibrated in the range from 0 to 95% RH. The calibration curves determined at IOS were later compared with the calibration curves that resulted in the best adjustment of the sensor signals to the actual level of gas during the validation tests (Figure 9).

IV. Testing Protocol at UTC

A test protocol was design to evaluate the main analytical characteristics of the three sensors under environmental conditions relevant to the PLSS. The testing protocol included the tests listed in Table 1.

Table 1.   Tests to be performed.

Test ID	Description	Parameter
2.1.1	Precision	CO_2
2.1.2	Recovery/hysteresis	CO_2
2.1.3	Response time	CO_2
2.1.4	Accuracy (deviation)	CO_2
2.1.5	Environmental conditions: balance gas	CO_2
2.1.6	Environmental conditions: pressure	CO_2
2.1.7	Environmental conditions: humidity	CO_2
2.1.8	Environmental conditions: flow rate	CO_2
2.1.9	Environmental conditions: temperature	CO_2
2.1.10	Precision	O_2
2.1.11	Recovery/hysteresis	O_2
2.1.12	Response time	O_2
2.1.13	Accuracy (deviation)	O_2
2.1.14	Environmental conditions: pressure	O_2
2.1.15	Environmental conditions: humidity	O_2
2.1.16	Environmental conditions: flow rate	O_2
2.1.17	Environmental conditions: temperature	O_2
2.1.18	Precision	H_2O
2.1.19	Recovery/hysteresis	H_2O
2.1.20	Response time	H_2O
2.1.21	Accuracy (deviation)	H_2O
2.1.22	Environmental conditions: balance gas	H_2O
2.1.23	Environmental conditions: pressure	H_2O
2.1.24	Environmental conditions: flow rate	H_2O
2.1.25	Environmental conditions: temperature	H_2O

The precision of a sensor can be calculated as the standard deviation of several consecutive readings of the sensor signal at a selected gas level. A test profile to evaluate that reading of repeatability was designed for five repetitions at each of four selected gas levels (Figure 2a shows the test profile for the CO_2 sensor). The hysteresis of a sensor can be calculated as the deviation on the sensor reading at a selected gas level, when the gas concentration increases and when it decreases. The test profile to evaluate hysteresis for the CO_2 sensors is shown in Figure 2b, and similar profiles were designed for the oxygen and humidity sensors. To evaluate the response time, we designed a test profile in which the gas level is varied between two selected levels as fast as the test rig allows. The test rig response time should be faster than the response time of the sensor system. After sensor calibration, the accuracy can be calculated as the deviation of the sensor reading from the actual value of gas concentration. The accuracy is usually calculated using certified cylinders of known concentration of the target gas. Accuracy can also be calculated as the deviation of the sensor readings from the reading from a traceable monitoring system, which are taken as the actual gas levels. The accuracy tests were initially designed assuming the use of certified gas cylinders. We designed a test profile that enabled us to average the sensor reading for a period of 30 minutes to calculate accuracy. Finally, the test protocols included several tests to evaluate the performance of the system under varying environmental conditions found in the PLSS, including the pure oxygen atmosphere, reduced pressure (Figure 2c), varying humidity (Figure 2d), varying temperature (Figure 2e) and, potentially, varying flow rate (Figure 2f).
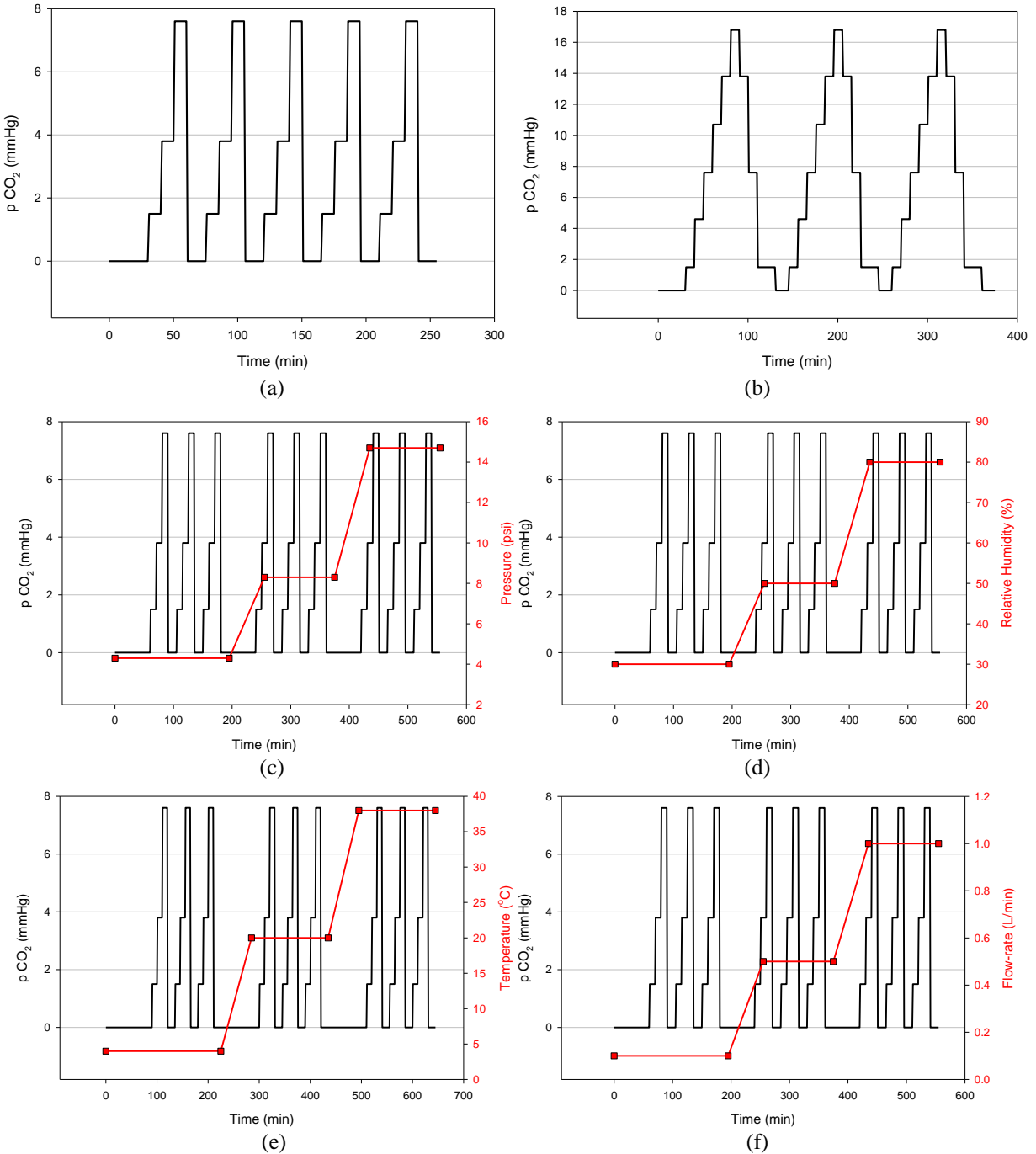
Figure 2. Nominal gas level and environmental condition profiles for characterizing the carbon dioxide sensor.

Tests were conducted according to the test protocol document, except where noted in the comments in Section VI. The sensors were valved off from the rest of the test setup between test points.

V. Test Facility at UTC

The testing of the MOGS units was conducted in two test setups at the UTC Aerospace Systems, Land and Sea (HS SL&S) Advanced Technology Engineering Laboratory. In the first setup we validated the humidity sensor, and in the second the carbon dioxide and oxygen detection.

A. Humidity Detection Setup

Humidity detection tests were conducted in a temporary laboratory setup with six water spargers submerged in five temperature controlled baths. A single six-way valve switched among the spargers, and a second valve selected dry nitrogen. The two sensors and their electronics were strapped to laboratory cold plates, which were controlled via another constant-temperature water bath. Flow rate was monitored on a float meter. Test set 2.1.25 was conducted with Pyropel insulation over the sensors, electronics, and cold plates. Test set 2.1.23 was conducted with a portable vacuum pump. Temperature and humidity data were collected in a laboratory data logger to compare with the MOGS data.

B. Carbon Dioxide and Oxygen Detection Setup

Carbon dioxide and oxygen detection tests were conducted on the Engineering Laboratory Subscale Air Rig, a permanent setup that can be modified and reprogrammed depending on the testing needs. The two sensors and their electronics remained strapped to laboratory cold plates. Flow rate was again monitored on a float meter. Levels of carbon dioxide and oxygen were controlled via inputs to mass flow meters. Carbon dioxide levels were measured with a Horiba carbon dioxide monitor that was part of the rig, and CO_2 data was recorded at each time step. Oxygen levels were measured with a portable oxygen analyzer that has only a digital display as its output. The display reads to the nearest tenth of a percent, and the readings were input into the test data stream manually. Humidity levels were controlled by the air rig, and input as dew point temperature. Tests 2.1.9 and 2.1.17 were conducted with Pyropel insulation over the sensors, electronics, and cold plates.

The sensors and their electronics were strapped to water-cooled cold plates and plumbed in series. The CO_2 and O_2 analyzers for the lab were calibrated with zero and span daily.

# VI.   Validation Tests at UTC Laboratory

This article first discusses the raw data collected (phase measurements), before processing and before signal compensation for temperature and humidity. Analyzing the raw data enables us to explain the effects of the environmental conditions on the sensor signal. Then we discuss the results obtained after processing the data, and calculating the gas levels for each of the three optical sensors.

C. Test Results: Raw Data (This should be A)

We reported the raw data below according to the order established in the test protocol, though the actual order of the tests was adjusted to simplify the experimental procedures. The tests to evaluate sensor hysteresis were omitted, but all other tests in the protocol were performed with no significant limitations. Though we discuss the raw data for all three sensors, we include here only the raw data for the carbon dioxide sensor as an example. Because the carbon dioxide sensor is the most complex of the three gas sensors, this still enables us to discuss the data collected for the other two sensors.

1.   Precision

We conducted the precision testing according to the test protocol, and observed no significant anomalies. The raw phase reading for the CO_2 sensor and the reading from the gas analyzers in the test rig are shown in Figure 3. Excellent repeatability (precision) was observed throughout the test. Similar results (good repeatability) were also observed for the oxygen and humidity sensors.
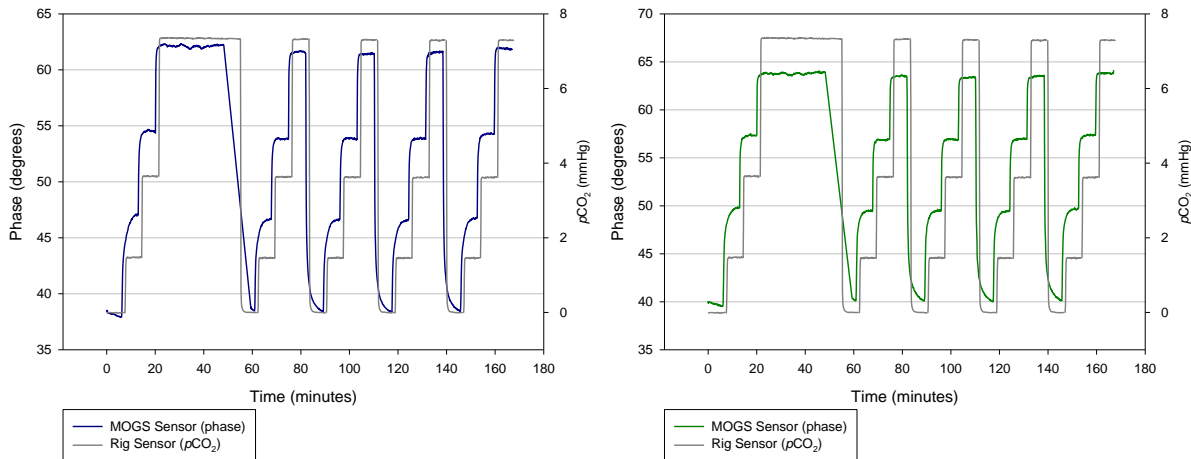
Figure 3. Response profile of the MOGS systems (phase) and rig sensor readings in Test 2.1.1 CO_2 Precision conducted at UTC: (a) MOGS v0.1-10 mm; (b) MOGS v0.1-5 mm.

2. Response Time

The raw phase reading for the CO_2 sensors and the reading from the gas analyzers in the test rig are shown in Figure 4. Similar sensor signal profiles were recorded for the oxygen and humidity sensors.
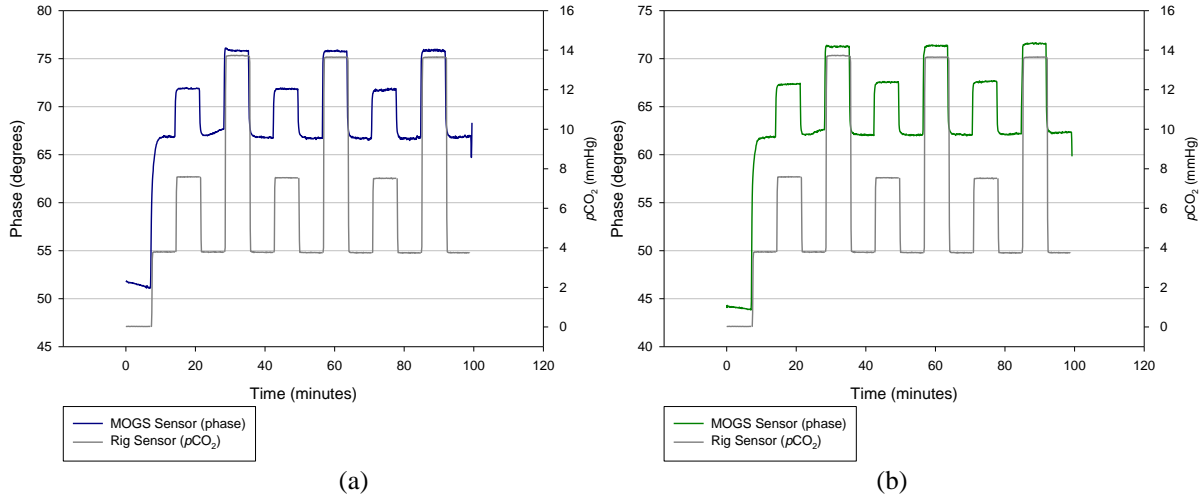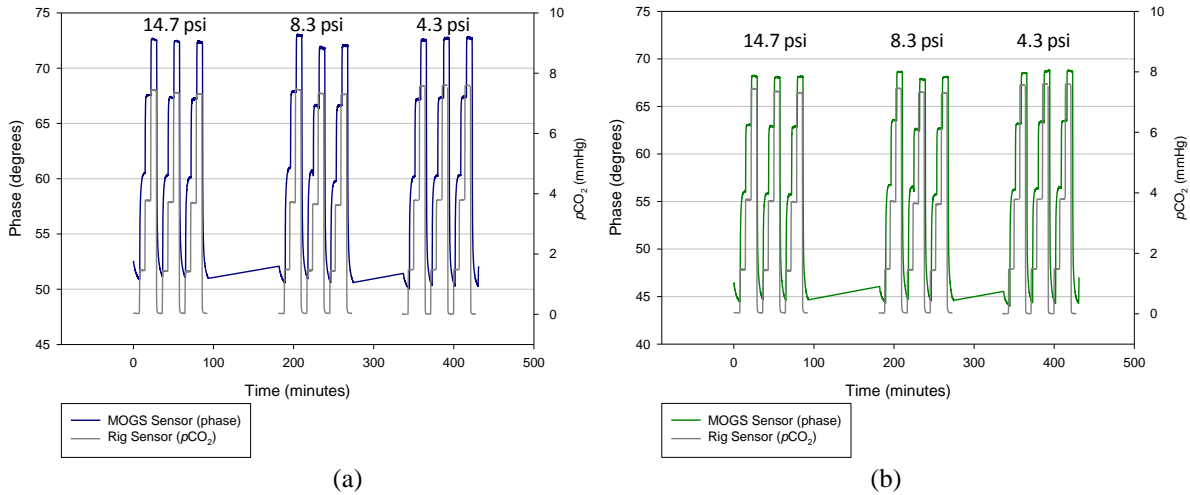

(a)   (b)

Figure 4. Response profile of the MOGS systems (phase) and rig sensor readings in Test 2.1.3 CO_2 Response Time conducted at UTC: (a) MOGS v0.1-10 mm; (b) MOGS v0.1-5 mm.

3. Balance Gas

This test was conducted using air as the balance gas for the CO_2 and humidity sensors. No differences in the sensor signal were observed between the tests conducted under nitrogen and the tests conducted under air for the CO_2 sensor, and minimal differences were observed for the humidity sensor. Tests were not conducted under pure oxygen, since the test rig used was not rated to operate under oxygen. However, since the data collected under air clearly shows no effect of the oxygen background in the sensor signal we can infer that the same result would have been observed under pure oxygen. No compensation of the sensor signal will be needed for the balance gas.

4. Pressure Effects

In this test, the CO_2 and oxygen levels were calculated to maintain the same partial pressures when the system was tested at 8.3 psi and at 4.3 psi as those during the ambient pressure tests. Humidity was controlled to the same dew points as in ambient pressure tests, maintaining the same partial pressure of water vapor, independent of the total pressure. The raw phase reading for the CO_2 sensors and the reading from the gas analyzers in the test rig are shown in Figure 5. No effect of the total pressure was observed in the sensor signals, so pressure compensation is not required. Similar results were recorded for the oxygen and humidity sensors, and in none of the sensors was pressure compensation applied.
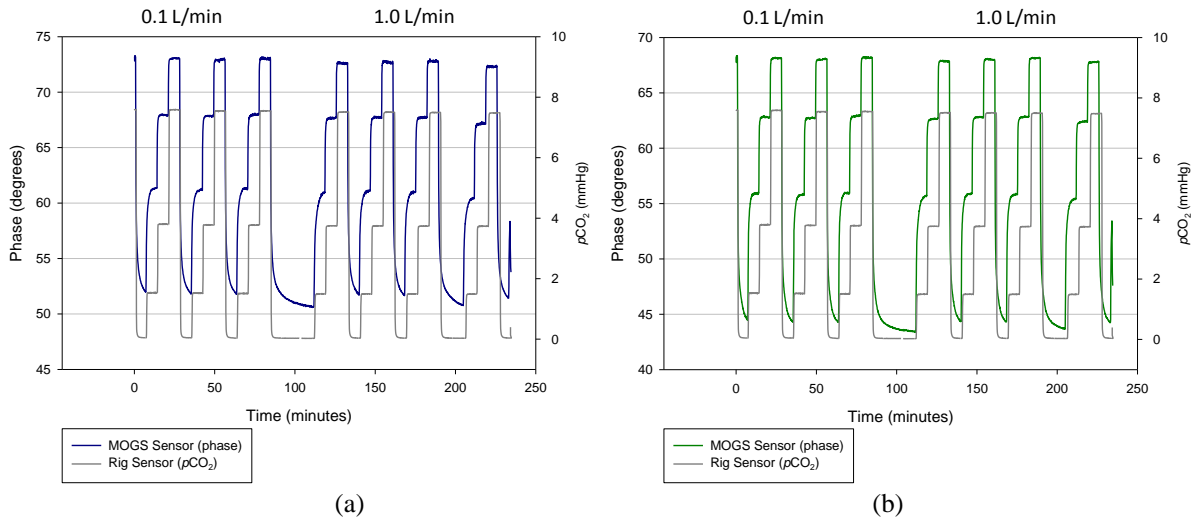
Figure 5. Response profile of the MOGS systems (phase) and rig sensor readings in Test 2.1.6 CO₂ Pressure Effects Gas conducted at UTC: (a) MOGS v0.1-10 mm; (b) MOGS v0.1-5 mm.

5. Humidity Effects

The oxygen and carbon dioxide sensors were tested at varying humidity. Tests were conducted according to the protocol, and the humidity was set by controlling the dew point. The raw phase reading for the CO_2 sensor and the reading from the gas analyzers in the test rig are shown in Figure 6. As reported previously, humidity affected the sensor response to carbon dioxide, and the phase values observed at the three humidity levels differ, so humidity compensation was applied (see Test Results: Processed Data below, after Figure 8) to calculate the CO_2 partial pressure from the phase values. For the oxygen sensor, we observed no effect of the humidity on the sensor response.
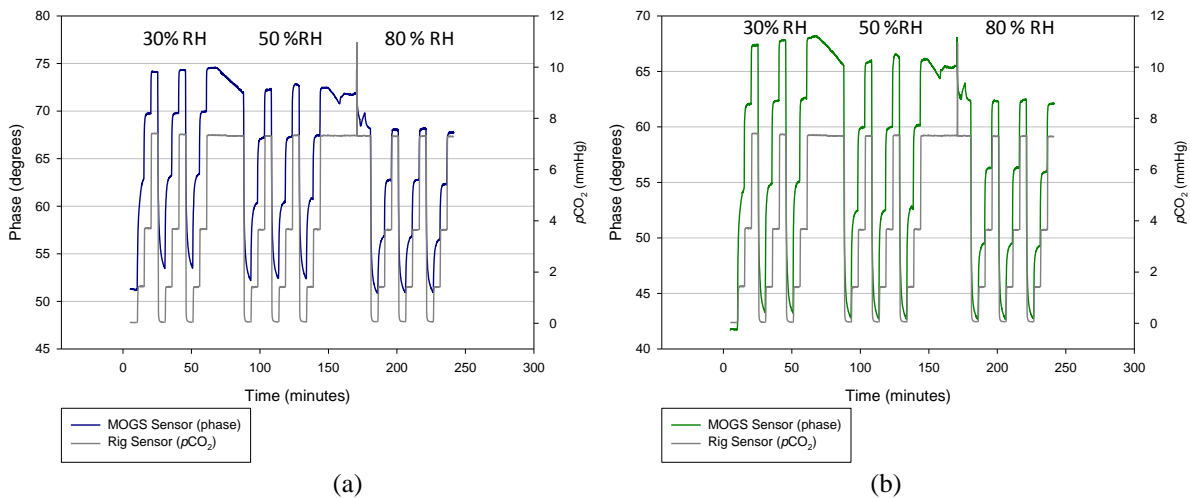
Figure 6. Response profile of the MOGS systems (phase) and rig sensor readings in Test 2.1.7 CO₂ Humidity Effects conducted at UTC: (a) MOGS v0.1-10 mm; (b) MOGS v0.1-5 mm.

6. Flow Rate Effects

The raw phase reading for the CO_2 sensor for this test and the reading from the gas analyzers in the test rig are shown in Figure 7. No effect of the flow rate on the sensor signals was observed for any of the three gas sensors, so flow rate control will not be required when the system is installed in a PLSS.
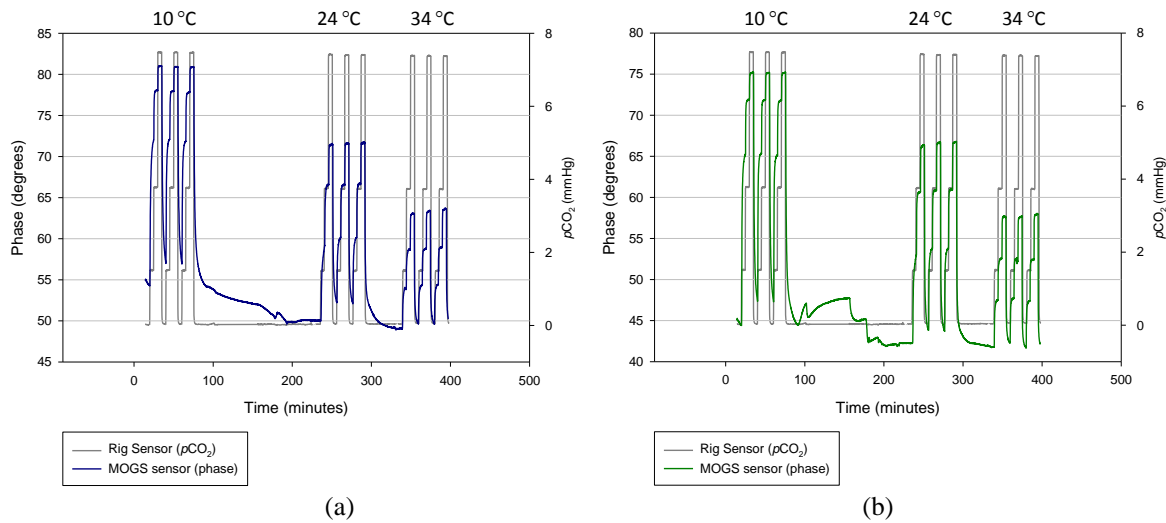
Figure 7. Response profile of the MOGS systems (phase) and rig sensor readings in Test 2.1.8 CO₂ Flow Rate Effects conducted at UTC: (a) MOGS v0.1-10 mm; (b) MOGS v0.1-5 mm.

7. Temperature Effects

The raw phase reading for the CO_2 sensors and the reading from the gas analyzers in the test rig are shown in Figure 8, for tests conducted at three temperatures. As reported above, temperature affected sensor sensitivity, so temperature compensation was applied (see Test Results: Processed Data). Similar results are observed for the humidity sensor signal, which depends significantly on the temperature. Temperature effects were also recorded for the oxygen sensor, but they were less significant than those for the CO_2 and humidity sensors.


Figure 8. Response profile of the MOGS systems (phase) and rig sensor readings in Test 2.1.9 CO₂ Temperature Effects conducted at UTC: (a) MOGS v0.1-10 mm; (b) MOGS v0.1-5 mm.

D. Test Results: Processed Data (This should be B)

The MOGS system can process the raw data (phase) in real time according to a pre-established calibration table, and generate measurements of the gas levels. However, for this study we applied the calibration algorithm offline, after all data was collected. Temperature readings from the test rig sensor were used for temperature compensation, instead of using the internal temperature sensor of the MOGS unit, since the sensors in the rig were more reliable, and evaluating temperature monitoring was not a study objective.

The two prototypes were calibrated at IOS before being shipped to the UTC facility. After calibration, the systems were disassembled and the readout unit, the optical cable, and the sensor flow-cell were packaged separately. The three modules were reassembled at UTC before the tests started. After this assembly, a quick test to

assure proper system operation was performed. That revealed the convenience of revising the calibration functions previously established at IOS. Using the data collected at ambient temperature in this initial quick test, the calibration matrixes were corrected for the humidity sensors in both units and for the oxygen sensor in unit MOGS v0.1-5 mm, before starting the tests included in the established protocol. Figure 9 shows the calibration function established initially at IOS and those for gas level calculation, determined from experimental data collected at UTC before starting the test protocol. The revised calibration functions do not differ significantly from those established at IOS, but this modification was necessary to achieve good correlation between the optical sensor systems and the standard sensors in the test rig.
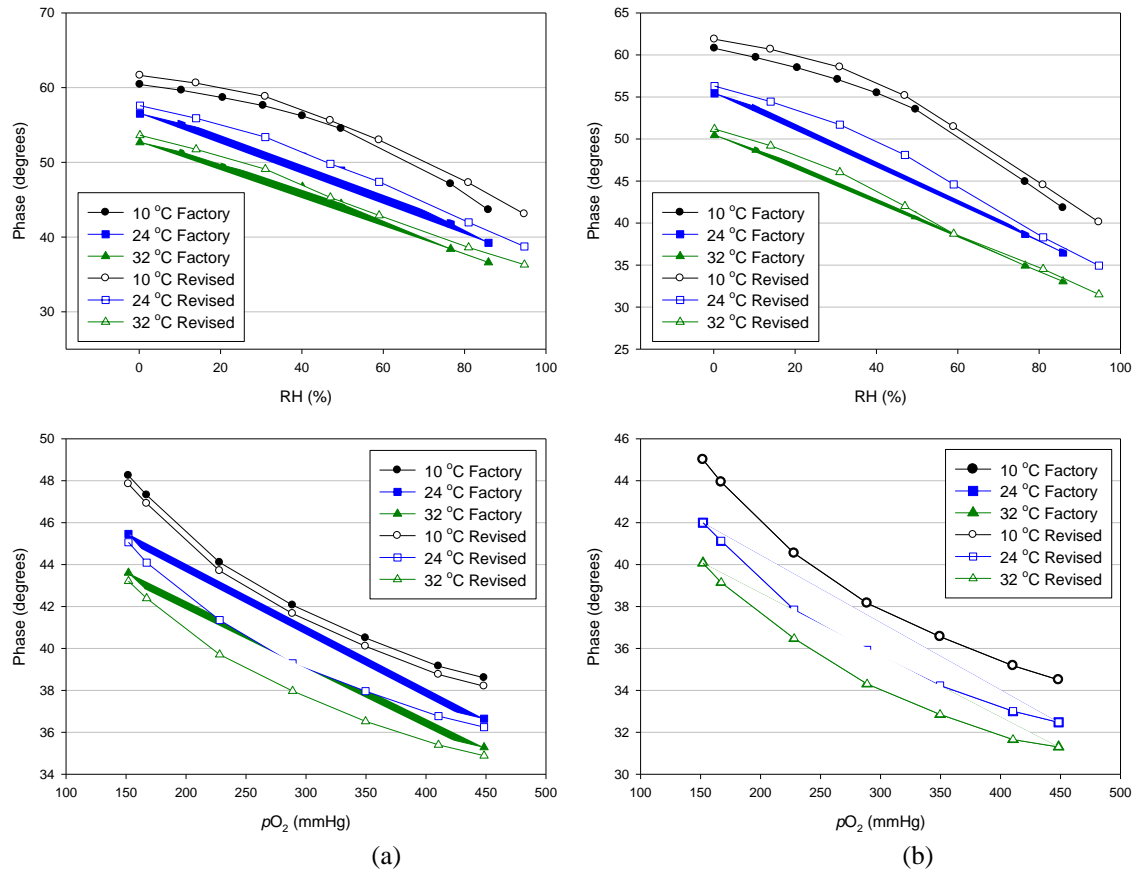
Figure 9. Calibration functions for the humidity and oxygen sensors established at IOS (factory) and established at UTC (revised): (a) MOGS v0.1-10 mm; (b) MOGS v0.1-5 mm.

This revision of the calibration functions for the humidity and oxygen sensors could have been avoided by revising the system assembly protocol and the design of the optical cable. These two corrections were implemented in a revised version of the MOGS system. In addition, the electronics unit was revised to reduce or even totally avoid the need for recalibration when the unit is disassembled and reassembled.

For the CO_2 sensors, a new calibration matrix was calculated based on the test conducted at varying humidity. Figure 10 compares the factory calibration matrix and the new calibration matrix calculated from the data collected at UTC for unit MOGS v0.1-10 mm. The significant differences observed between the two sets of functions result from instability of the CO_2 sensor elements, and not from instrumental causes. We are studying how to modify the CO_2 sensor elements so as to extend the life of the sensors and reduce or avoid the need for recalibration, and the results will be documented in future presentations.
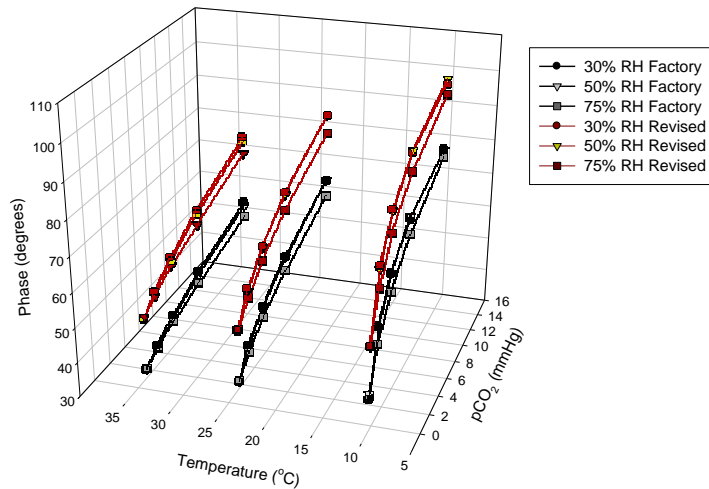
Figure 10.   Calibration functions for the carbon dioxide sensor in unit MOGS v0.1-10 mm established at IOS (factory) and established at UTC (revised).

The gas level calculated for each tests according to the revised functions, and the data recorded by the sensors in the test rig, are listed below in the order in which the tests were conducted.

E. Humidity Sensor Validation (This should be C)

8. H_2O Precision (This should be 1)

The readings from the MOGS system humidity sensors and the gas analyzers in the test rig are compared in Figure 11. Excellent correlation between the fiber optic sensor readings and the data from the rig sensor was observed for both MOGS units. Some deviation was observed at low humidity with dry gas. It appears that the slow response of the dew point meter in the rig, particularly at low humidity, was responsible for the observed deviation. This effect was observed throughout all the tests conducted to evaluate the optical humidity sensors, but completely dry gas (RH <5%) is not expected in the PLSS. Precision was calculated as the standard deviation of the five consecutive measurements at 28% RH and at 57% RH, which were the two humidity levels at which the test rig was most stable throughout the tests, and yielded values of 0.2% RH and 0.5% RH, respectively.


(a)   (b)
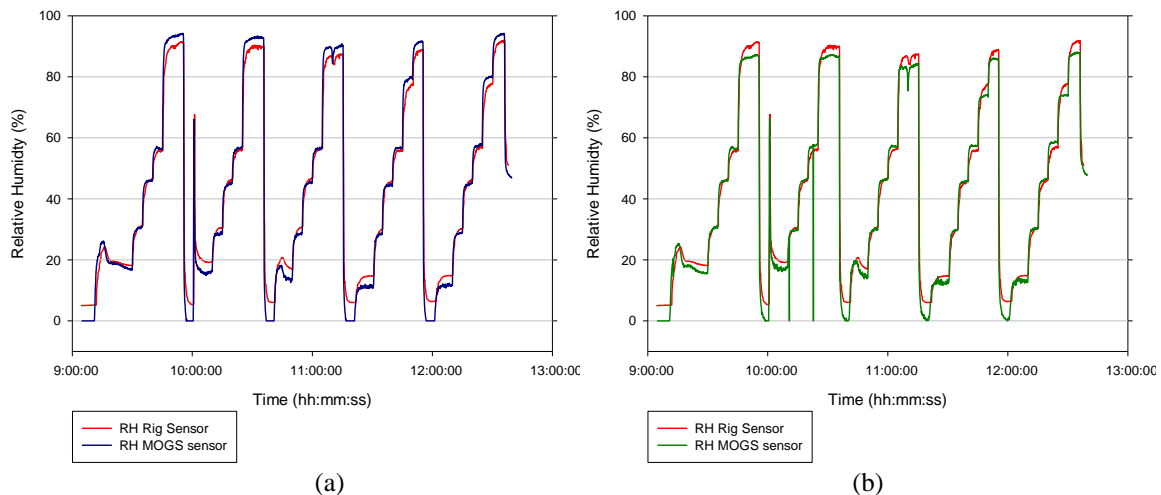
Figure 11.   MOGS systems and rig sensor readings in Test 2.1.18: (a) MOGS v0.1-10 mm; (b) MOGS v0.1-5 mm.

9. H_2O Balance Gas Effects

We conducted H_2O balance gas testing with air as the balance gas. The readings from the MOGS system humidity sensors and the gas analyzers in the test rig are compared in Figure 12. Excellent correlation between the

fiber optic sensor readings and the data from the rig sensor was observed for both MOGS units. No compensation for oxygen was applied; accuracy at low humidity levels could be improved by operating the humidity sensors in two modes of operation—nitrogen mode and oxygen mode (for air or pure oxygen).
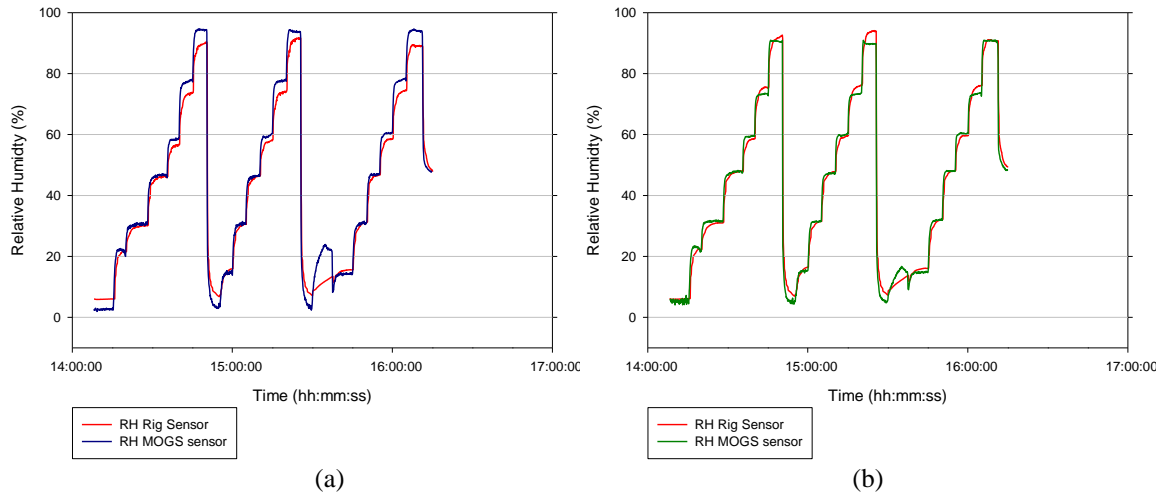
Figure 12.   MOGS systems and rig sensor readings in Test 2.1.22: (a) MOGS v0.1-10 mm; (b) MOGS v0.1-5 mm.

10. H₂O Response Time

The readings from the MOGS system humidity sensors and the gas analyzers in the test rig are compared in Figure 13. As expected, the MOGS humidity sensors were much faster than the rig sensor. From the data we can conclude that the observed response speed of the optical sensor (response time <6 s) was limited by the response speed of the test rig, and the actual sensor response time could be faster than that. Both units met the 10 s requirement for humidity monitoring in the PLSS.
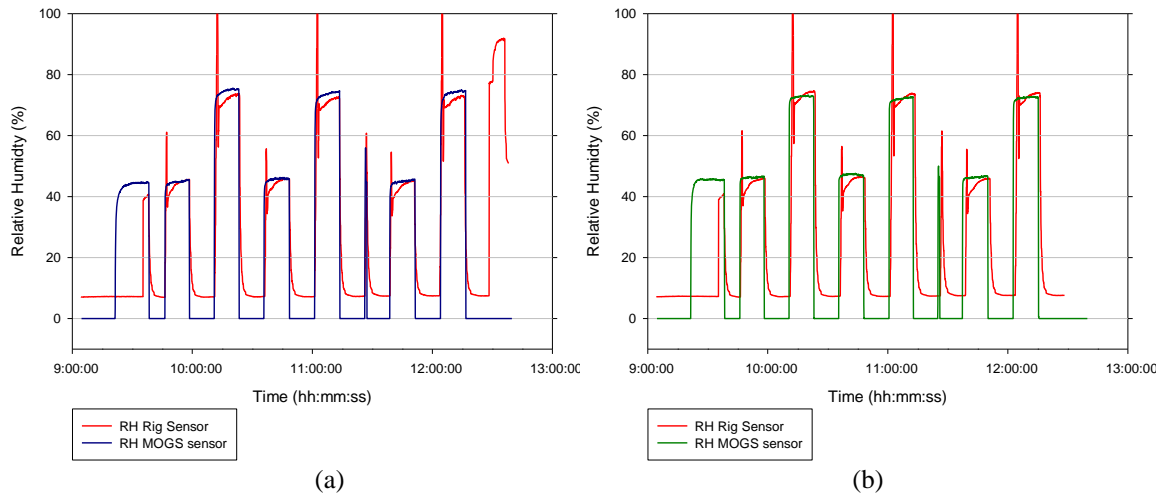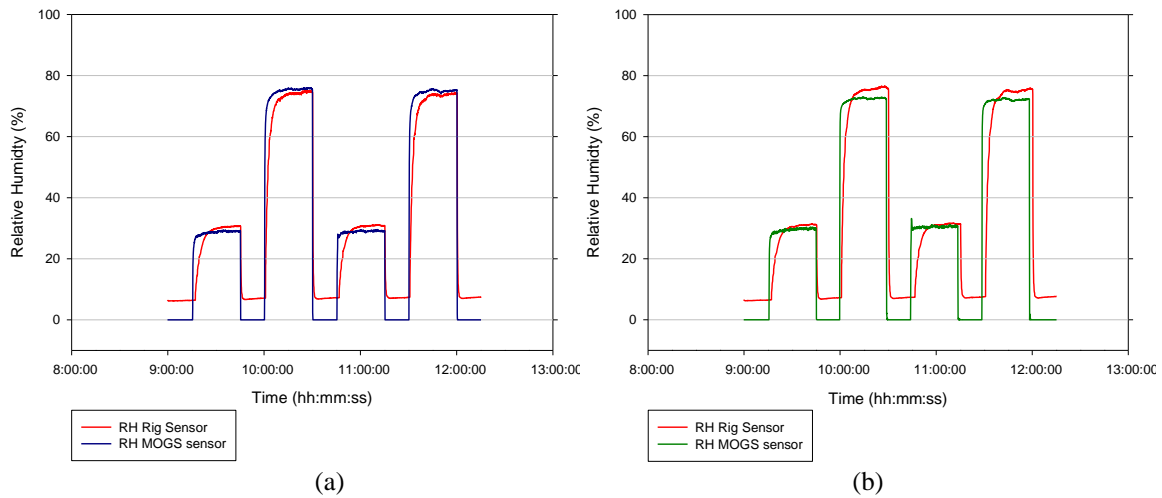

Figure 13.   MOGS systems and rig sensor readings in Test 2.1.20: (a) MOGS v0.1-10 mm; (b) MOGS v0.1-5 mm.

11. H₂O Accuracy

The readings from the MOGS system humidity sensors and the gas analyzers in the test rig are compared in Figure 14. Excellent correlation between the fiber optic sensor readings and the data from the rig sensor was observed for both MOGS units. The deviation was 1% RH at 30% RH and 75% RH for unit MOGS v0.1-10 mm (blue trace). The deviation was 2% RH at 30% RH and 4% RH at 75% RH for unit MOGS v0.1-5 mm (green trace). As explained above, with dry gas the slow response of the humidity sensor in the test rig is responsible for the deviation observed. In addition, the calibration algorithm applied in the MOGS is programmed to calculate 0% RH

when the humidity level are below 5% RH. Both systems met the requirements for humidity monitoring in the PLSS (deviation < 5% RH).

(a)   (b)

Figure 14.   MOGS systems and rig sensor readings in Test 2.1.21: (a) MOGS v0.1-10 mm; (b) MOGS v0.1-5 mm.
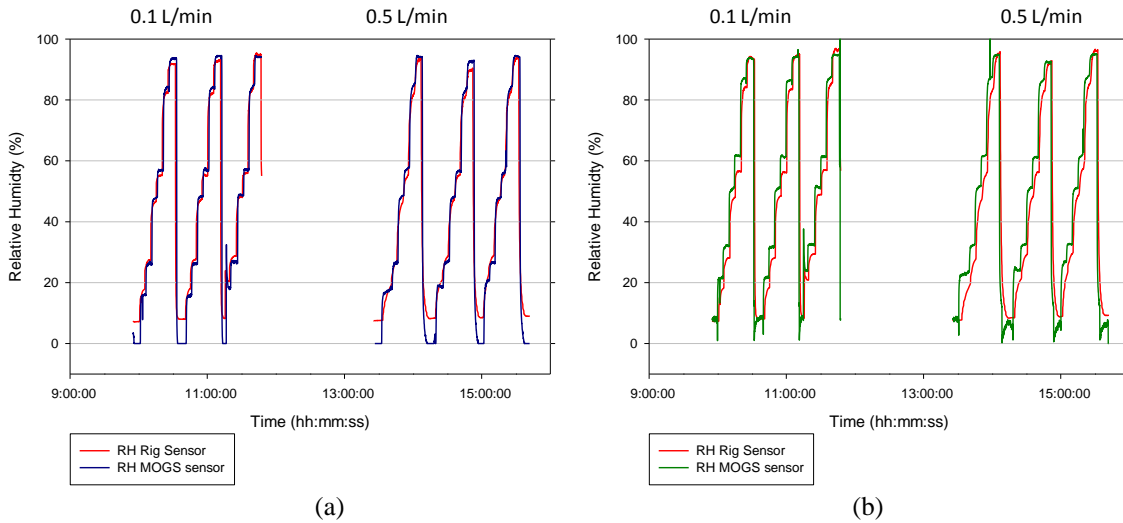
12. H_2O Temperature Effects

Tests were conducted according to the protocol, with some modifications to avoid having water condense in the test rig. The readings from the MOGS system humidity sensors and the gas analyzers in the test rig are compared in Figure 15. Temperature compensation was applied. Good correlation between the fiber optic sensor readings and the data from the rig sensor was observed for both MOGS units. However, the deviation observed at 34°C for unit MOGS v0.1-10 mm (blue trace), visually greater than at low temperature, suggests that the temperature compensation parameters must be revised.

(a)   (b)
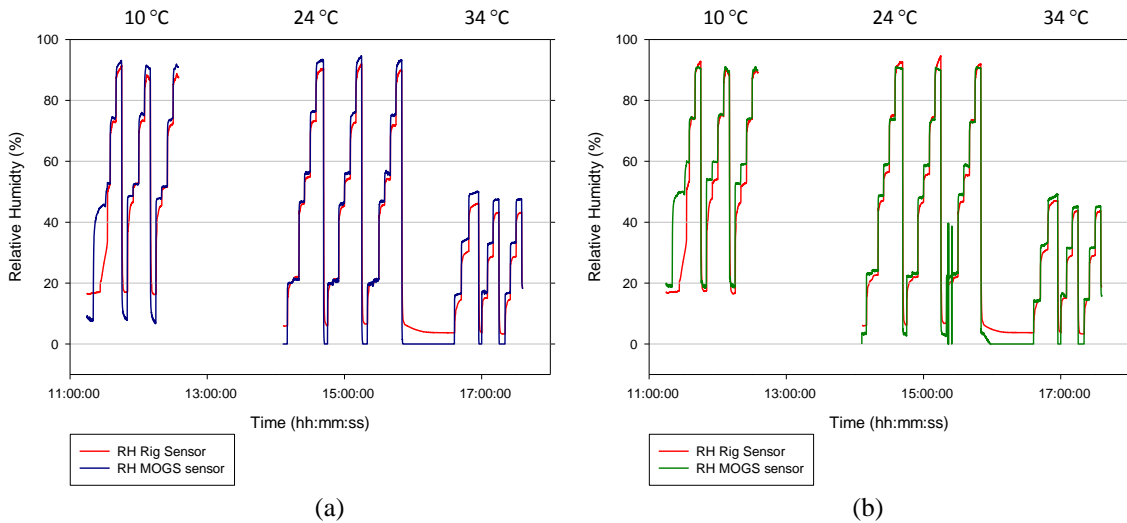
Figure 15.   MOGS systems and rig sensor readings in Test 2.1.25: (a) MOGS v0.1-10 mm; (b) MOGS v0.1-5 mm.

13. H_2O Flow Rate Effects

The readings from the MOGS system humidity sensors and the gas analyzers in the test rig are compared in Figure 16. Excellent correlation between the fiber optic sensor readings and the data from the rig sensor was observed for both MOGS units, without applying any compensation to the raw sensor signal.

Figure 16.   MOGS systems and rig sensor readings in Test 2.1.24: (a) MOGS v0.1-10 mm; (b) MOGS v0.1-5 mm.

14. H₂O Pressure Effects

Tests were conducted according to the protocol, and dew point was held constant to maintain the partial pressure of water vapor, even at reduced total pressure. The readings from the MOGS system humidity sensors and the gas analyzers in the test rig are compared in Figure 17. Excellent correlation between the fiber optic sensor readings and the data from the rig sensor was observed for the MOGS v0.1-10 mm unit (blue trace). No pressure compensation was applied. The humidity sensor in unit MOGS v0.1-5 mm was out of calibration before starting the test. Examination of the sensor unit after finalizing the tests suggests that the problem was caused by a loose optical connector. The design of the optical connectors has since been revised to prevent this problem in the future. Readings from the humidity sensor in unit MOGS v0.1-5 mm were not accurate in any of the tests conducted after this test, including the tests conducted to evaluate the CO_2 sensor performance.
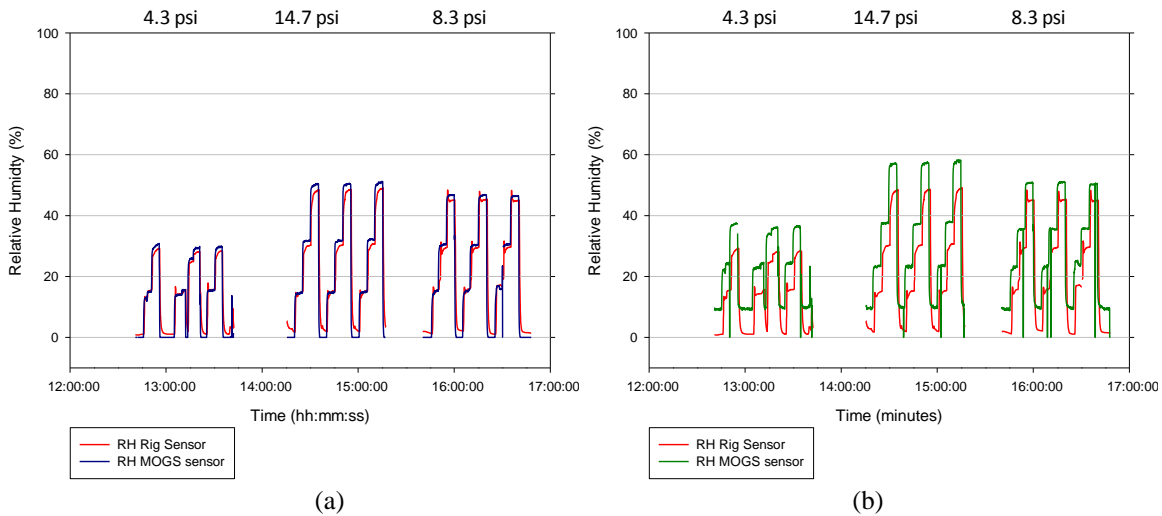
Figure 17.   MOGS systems and rig sensor readings in Test 2.1.23: (a) MOGS v0.1-10 mm; (b) MOGS v0.1-5 mm.

F. Carbon Dioxide Sensor Validation

As described above, the humidity sensor in unit MOGS v0.1-5 mm became inaccurate after Test 2.1.23, so humidity compensation for the CO_2 sensors in that unit created deviation in the CO_2 readings. For that reason, the processed data for the CO_2 sensor in unit MOGS v0.1-5 mm is not discussed in detail. A change was needed in the

calibration parameters for the CO_2 sensors after Test 2.1.1 CO_2 Precision. In order to record all CO_2 data processed with the same set of calibration parameters, Test 2.1.1 is not included in the discussion.

15. CO$_2$ Humidity Effects

The readings from the MOGS v0.1-10 mm CO_2 sensor and the gas analyzers in the test rig are compared in Figure 18. When humidity compensation was applied, excellent correlation between the fiber optic sensor readings and the data from the rig sensor was observed, at the three selected humidity levels. However, during the periods when humidity was changing between 30% RH and 50% RH and between 50% RH and 80% RH, the sensor did not maintain good accuracy. Changes in humidity affect the CO_2 sensor response several seconds later than they actually occur, and this was not considered in the calibration algorithm. An advanced algorithm for humidity compensation that takes this into account is necessary. Precision was calculated as from the data collected in this test, and the CO_2 sensors exhibited excellent precision of 0.1 mmHg or better at the gas levels tested.

16. CO$_2$ Temperature Effects

The readings from the MOGS v0.1-10 mm CO_2 sensor system and the gas analyzers in the test rig are compared in Figure 18. Once temperature compensation was applied, excellent correlation between the fiber optic sensor readings and the data from the rig sensor was observed for most of the test. Deviation of 0.9 mmHg was observed at 24°C at pCO$_2$ 7.5 mmHg, while for the same partial pressure the deviation is below 0.2 mmHg at 10°C and at 34°C. The linear interpolation for temperature compensation is considered responsible for that difference in deviation at these temperatures, which indicates the need of revising the temperature compensation algorithm for this sensor.
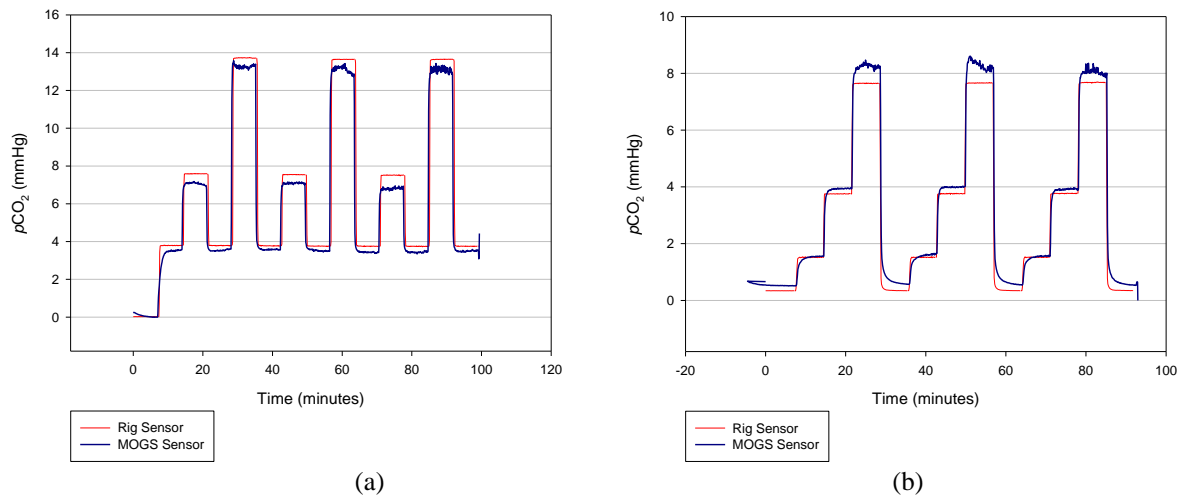

(a)   (b)
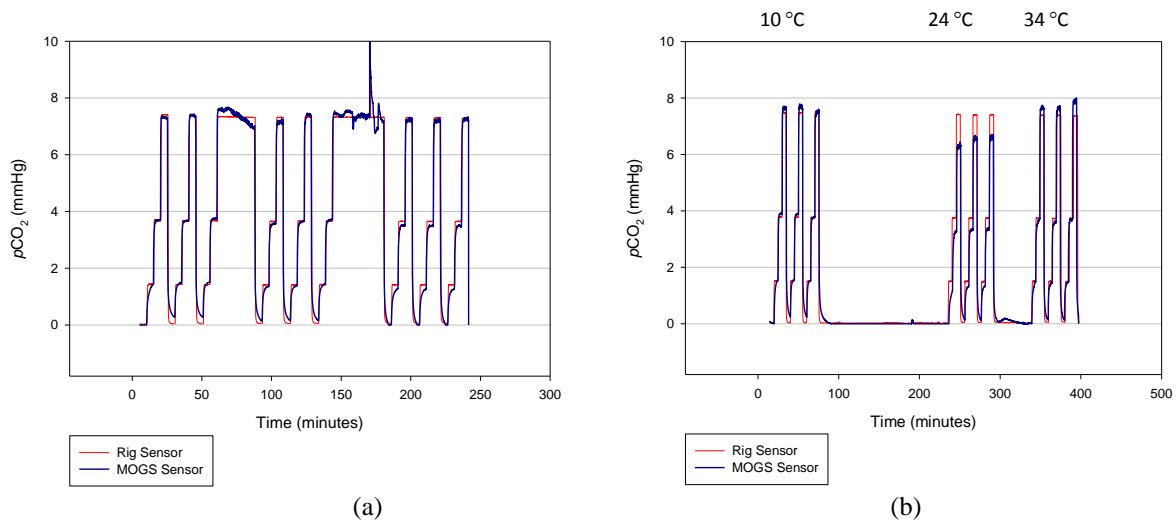
Figure 18. MOGS v0.1-10 mm CO₂ sensor and rig sensor readings in (a) Test 2.1.7 and (b) Test 2.1.3.

17. CO$_2$ Response Time

The readings from the MOGS v0.1-10 mm CO_2 sensor and from the gas analyzers in the test rig are compared in Figure 19. The calculated response time was 10-12 s from 4 to 7 mmHg and from 4 to 13 mmHg. The calculated inverse response time was ~12-15 s from 7 to 4 mmHg and from 13 to 4 mmHg. The requirement for the CO_2 sensor in the PLSS is a response time of 8 s. Thinner sensor films will be fabricated to meet that response time requirement.

18. CO$_2$ Balance Gas

The readings from the MOGS v0.1-10 mm CO_2 sensor and the gas analyzers in the test rig are compared in Figure 19. Good correlation between the fiber optic sensor readings and the data from the rig sensor was observed, when air was used instead of nitrogen as the balance gas and no compensation was applied.

Figure 19.   MOGS v0.1-10 mm CO$_2$ sensor and rig sensor readings in (a) Test 2.1.3 and (b) Test 2.1.5.

19. CO$_2$ Flow Rate Effects

The readings from the MOGS v0.1-10 mm CO$_2$ sensor and the gas analyzers in the test rig are compared in Figure 20. Excellent correlation between the fiber optic sensor readings and the data from the rig sensor was observed at both flow rates without any compensation.

20. CO$_2$ Pressure Effects

The readings from the MOGS v0.1-10 mm CO$_2$ sensor and the gas analyzers in the test rig are compared in Figure 20. Excellent correlation between the fiber optic sensor readings and the data from the rig sensor was observed at the three total pressure values. Compensation by pressure was not applied.
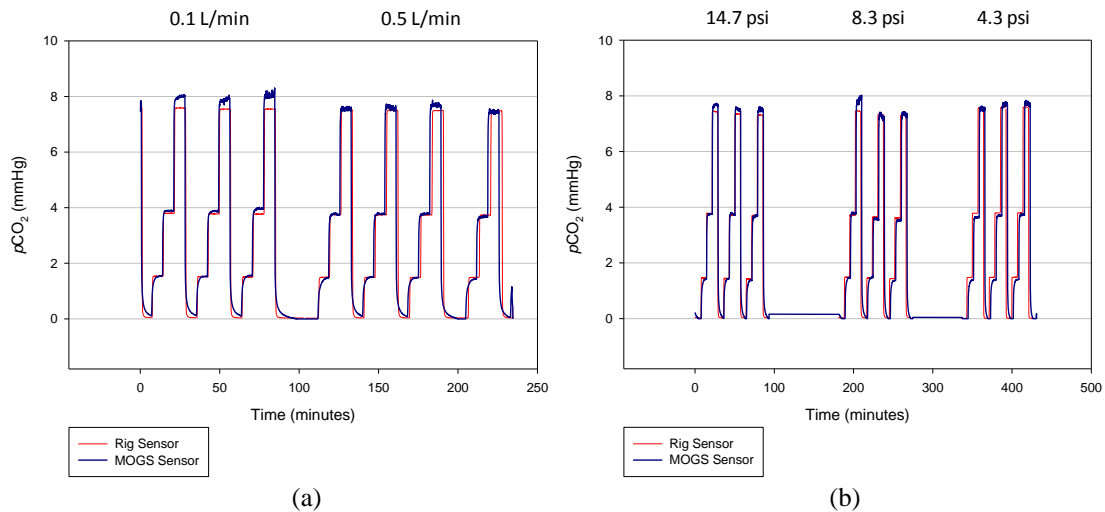
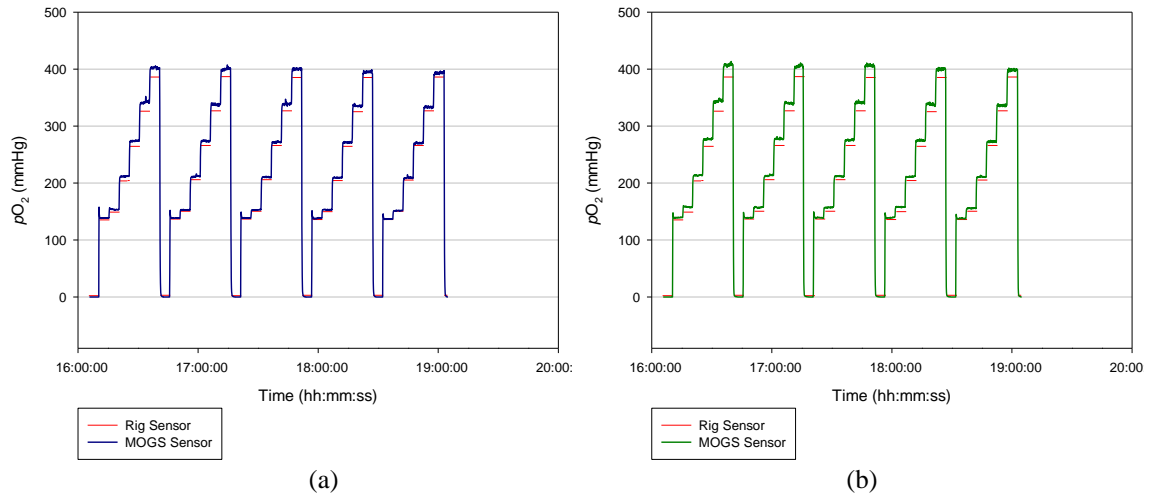Figure 20.   MOGS system SN001 and rig sensor readings in (a) Test 2.1.8 and (b) Test 2.1.6.

G. Oxygen Sensor Validation

21. O$_2$ Precision and Accuracy

The readings from the MOGS system sensors and from the gas analyzers in the test rig for this test are compared in Figure 21. Good correlation between the fiber optic sensor readings and the data from the rig sensor was observed. Deviation from the actual pO$_2$ value (reading from the test rig oxygen sensor) of 3 mmHg in the low range of oxygen up to 220 mmHg was observed (this range corresponds to an EMU operating at 4.3 psi). Deviation was also 3 mmHg up to 10 mmHg at higher pO$_2$ for the MOGS v0.1-10 mm, and was up to 19 mmHg for the MOGS v0.1-5 mm (this oxygen range corresponds to a EMU operating at 8.3 psi). The repeatability of the oxygen sensor was excellent, with precisions of 1 mmHg in the lower pO$_2$ range and 3.5 mmHg or better in the upper pO$_2$ range,

for both systems. This observation suggests that improved calibration functions or protocols could enhance accuracy and improve deviation, since the sensor precision was significantly lower than the deviation. In any case, the oxygen optical sensor will exhibit better performance in an EMU operating at lower pressure under pure oxygen, than in an EMU operating under oxygen at higher total pressure values.

(a)   (b)

Figure 21.   MOGS systems and rig sensor readings in Test 2.1.10: (a) MOGS v0.1-10 mm; (b) MOGS v0.1-5 mm.
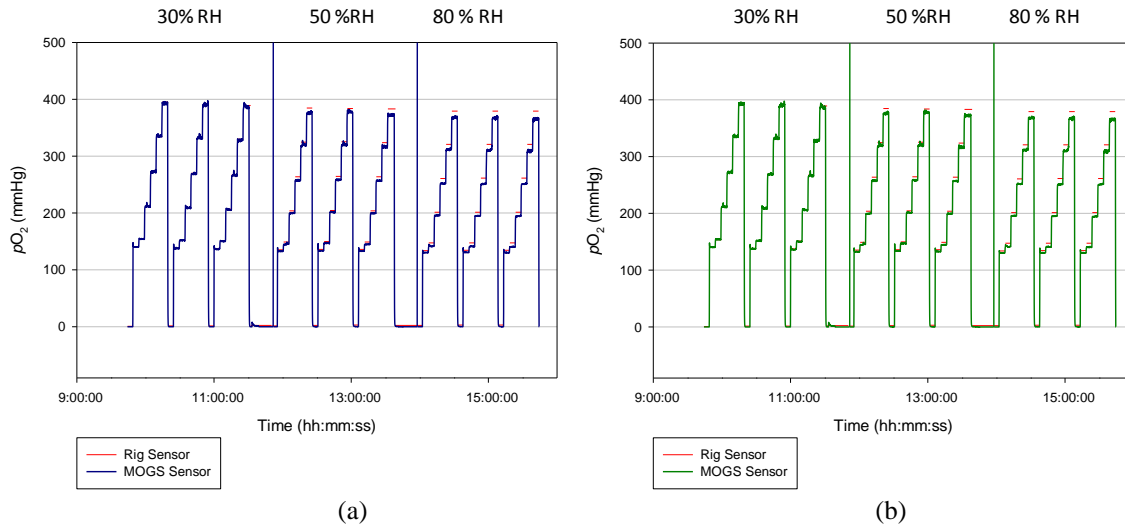
22. O₂ Temperature Effects

The readings from the MOGS system sensors and the gas analyzers in the test rig are compared in Figure 22. Good correlation between the fiber optic sensor readings and the data from the rig sensor was observed, with compensation of the sensor signal for temperature.

(a)   (b)
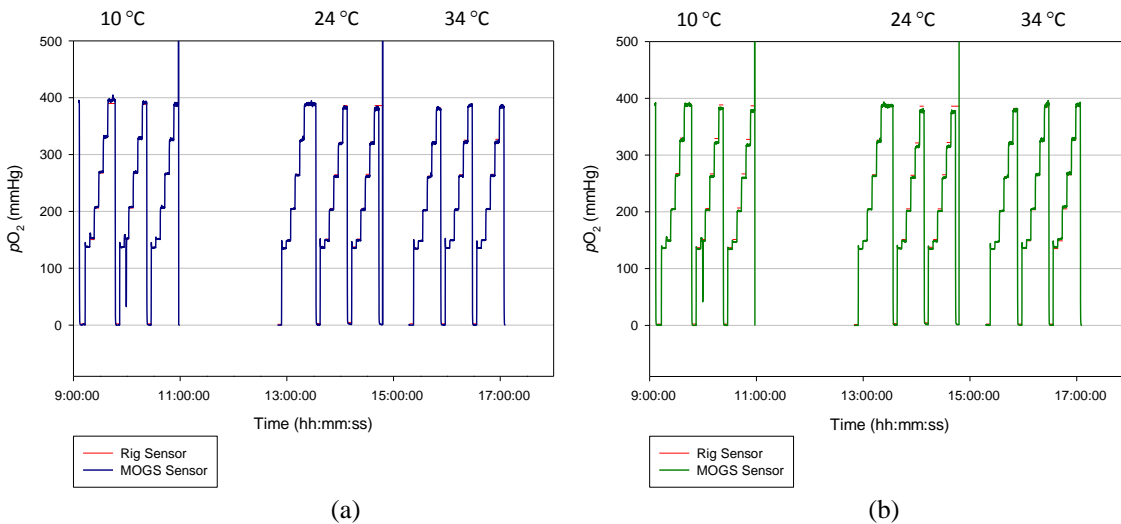
Figure 22.   MOGS systems and rig sensor readings in Test 2.1.17: (a) MOGS v0.1-10 mm; (b) MOGS v0.1-5 mm.
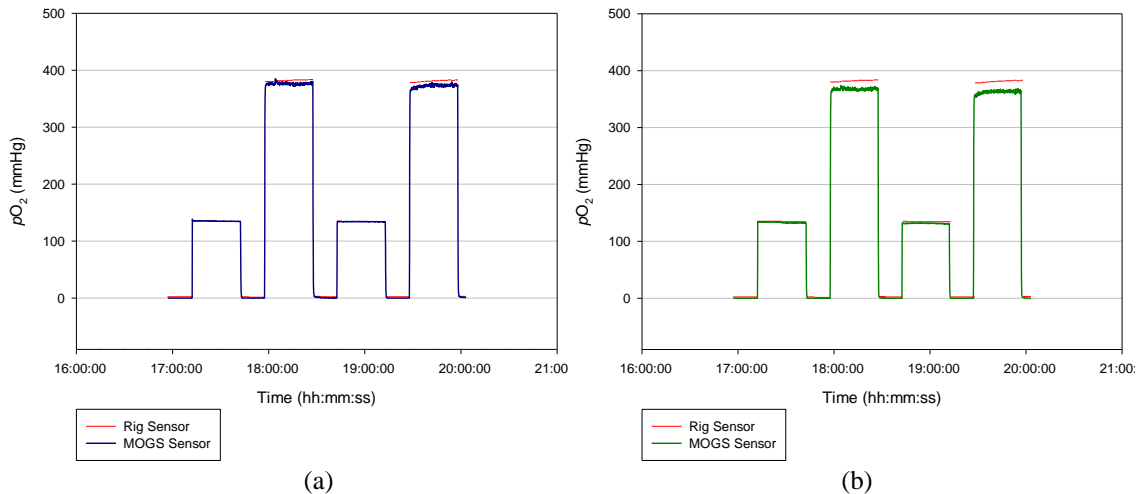
23. O₂ Humidity Effects

The readings from the MOGS system sensors and from the gas analyzers in the test rig are compared in Figure 23. Good correlation between the fiber optic sensor readings and the data from the rig sensor was observed, even with no compensation for humidity.

Figure 23.   MOGS systems and rig sensor readings in Test 2.1.15: (a) MOGS v0.1-10 mm; (b) MOGS v0.1-5 mm.
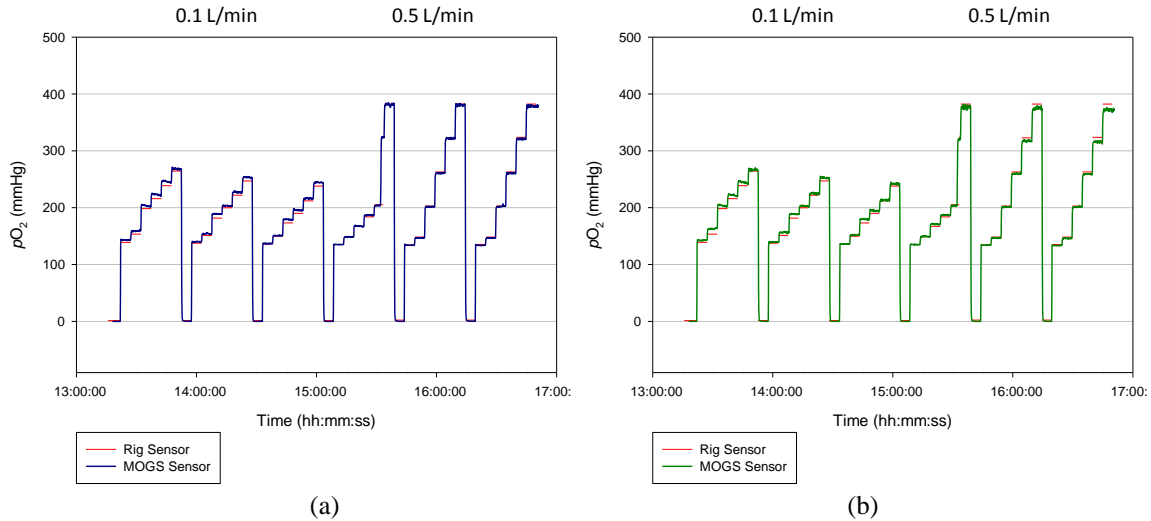
24. O₂ Accuracy

The readings from the MOGS system sensors and the gas analyzers in the test rig are compared in Figure 24. Excellent correlation between the fiber optic sensor readings and the data from the rig sensor was observed. The deviation was 0.9% (1 mmHg) at 135 mmHg and 1.5% (6 mmHg) at 380 mmHg for unit MOGS v0.1-10 mm (blue trace). The deviation was 0.9% (1 mmHg) at 135 mmHg and 3.0% (12 mmHg) at 380 mmHg for unit MOGS v0.1-5 mm (green trace). Both met the requirements for oxygen monitoring in the PLSS. As explained during the discussion of the data collected in the precision tests, the deviation could be reduced by applying improved calibration protocols.

Figure 24.   MOGS systems and rig sensor readings in Test 2.1.13: (a) MOGS v0.1-10 mm; (b) MOGS v0.1-5 mm.

25. O₂ Flow Rate Effects

Oxygen partial pressures above 300 mmHg were not generated during the tests conducted at 0.1 L/min., because of a problem in the oxygen regulator valve, which was later resolved and the tests at 0.5 L/min., were conducted as planned, reaching higher partial pressures of oxygen. The readings from the MOGS system sensors and the gas analyzers in the test rig are compared in Figure 25. Excellent correlation between the fiber optic sensor readings and the data from the rig sensor was observed, with no effect of the gas flow rate observed, and no compensation applied to the raw signal.

Figure 25.   MOGS systems and rig sensor readings in Test 2.1.16: (a) MOGS v0.1-10 mm; (b) MOGS v0.1-5 mm.

26. O$_2$ Pressure Effects

O$_2$ pressure effects could only be tested at very low oxygen concentrations, because the vacuum pumps available were not rated for oxygen concentrations >30%. O$_2$ partial pressures of 30 and 60 mmHg were selected for the reduced pressure tests. The readings from the MOGS system sensors and the gas analyzers in the test rig are compared in Figure 26. Good correlation between the fiber optic sensor readings and the data from the rig sensor was observed, with no pressure compensation.
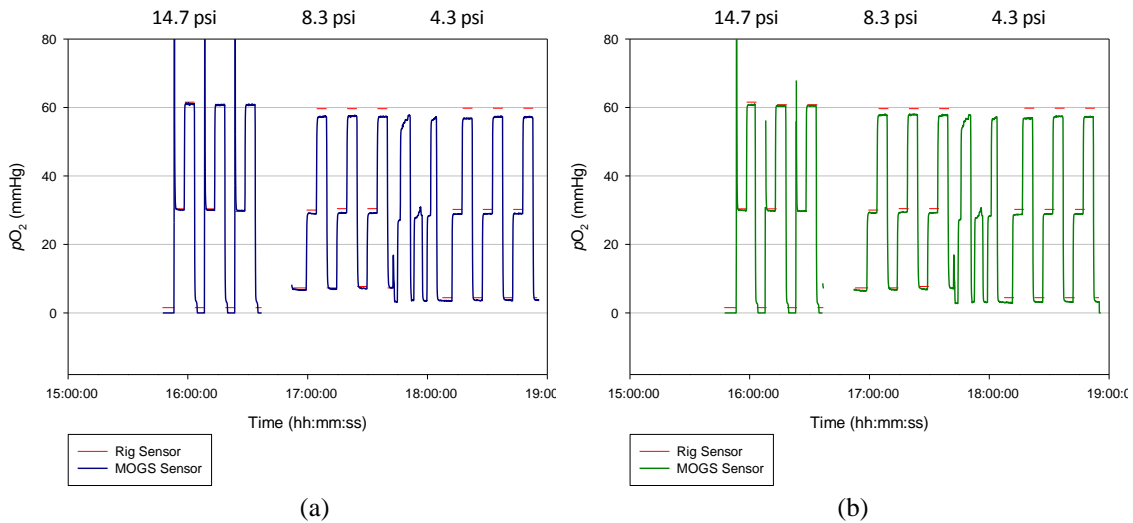
Figure 26.   MOGS systems and rig sensor readings in Test 2.1.14: (a) MOGS v0.1-10 mm; (b) MOGS v0.1-5 mm.

VII.   Conclusions

Intelligent Optical Systems has developed a compact gas monitor incorporating luminescence sensor elements for carbon dioxide, oxygen, and humidity monitoring, and the analytical characteristics of two prototypes were evaluated through a set of tests conducted at a UTC laboratory. The readout optoelectronic unit is a compact phase-resolved luminescence detector connected through an optical cable to a gas flow-through cell enclosing the luminescent sensors. The monitoring system is being developed as a candidate sensor module for the advanced PLSS under development at JSC.

A test plan was generated to evaluate precision, accuracy, response time, and environmental effects, considering the balance gas, temperature, humidity, pressure, and flow rate for each of the sensors, and the two prototypes were

evaluated according to the test plan, which included tests at the environmental conditions and ranges relevant to the PLSS.

The humidity and oxygen sensors required a calibration correction before starting the characterization tests at UTC, which were based on the data collected in a quick calibration test. This calibration revision could be avoided by revising the system assembly protocol and the design of the optical cable. (Both revisions have been implemented in the next generation system.)

The CO_2 sensors required extensive revision of the calibration functions. This limitation was due to a lack of stability of the CO_2 sensor elements, which can only be resolved by designing a new sensor material.

Once the system prototypes were calibrated, throughout the extensive testing, all three sensors readings exhibited good correlation with the data collected with the standard analyzers incorporated in the test rig, which were calibrated daily against certified standard gas cylinders.

The humidity sensors exhibited precision of 0.5% RH or better, and deviation below 5% RH. No effect of total pressure or flow rate was observed, and neither compensation nor control of either one would be required for operation in a PLSS. Operation under oxygen atmosphere was also demonstrated. Temperature compensation was applied. Significant thermal effect on the sensor response can be consider a disadvantage of the luminescence humidity sensors in comparison with classical humidity sensor materials, but proper temperature compensation can be used, in order to meet the requirements of sensors for the PLSS. Response faster than that of the laboratory analyzers was demonstrated.

The oxygen sensors exhibited precision of 1 mmHg or better at the low rage of pO_2, which would correspond with a PLSS operating at 4.3 psi total pressure and precision of 3 mmHg or better at the oxygen range that would correspond with a PLSS operating at 8.3 psi. The deviation with the actual oxygen levels was up to 19 mmHg at 400 mmHg, which is 5% of the reading. Fast response and no effect of humidity, total pressure or flow rate were demonstrated. Temperature compensation was applied, though the thermal effect is not as significant as for the humidity sensors.

The CO_2 sensors exhibited excellent precision of 0.1 mmHg or better at the 0.0 to 7.5 mmHg pCO_2 range. Deviation from the laboratory analyzer readings was lower than 1 mmHg throughout the tests. As with the other sensors, operation under oxygen was demonstrated, with no effect of total pressure or flow rate on the sensor signals.

Based on the results of these tests, accuracy can be improved by revising the calibration algorithms for calculating the gas levels from the raw sensor signal. Some reliability problems were also identified, which were characteristic of the stage of development of the prototypes tested, and which were resolved in a revision of the system assembly.

This technology reduces size and power requirements in comparison to IR-based devices, and it can operate under liquid water condensation, a condition at which the IR-based sensors in the ISS EMU PLSS are seriously compromised. However, stable calibration funtions over time is still to be demonstrated, as is reliability comparable to that of the IR sensors.

Acknowledgments

References

[1] Dietrich, D., Paul, H., and Conger, B., "Evaluation of Carbon Dioxide Sensors for the Constellation Space Suit Life Support System for Surface Exploration," SAE Technical Paper 2009-01-2372, 2009, doi:10.4271/2009-01-2372.

[2] Swickrath, M., Anderson, M., McMillin, S., and Broerman, C., "Application of Commercial Non-Dispersive Infrared Spectroscopy Sensors for Sub-ambient Carbon Dioxide Detection," *42nd International Conference on Environmental Systems*, AIAA 2012-3454, San Diego, CA, 2012.

[3] International Space Station (ISS) EVA Suit Water Intrusion High Visibility Close Call IRIS Case Number: S–2013–199–00005, National Aeronautics and Space Administration.

[4] Mills, A., Eaton, K., "Optical Sensors for Carbon Dioxide: An Overview of Sensing Strategies Past and Present," *Quim. Anal.* (Barcelona), Vol. 19, Supl. 1, 2000, pp. 75-86.

[5] Delgado J., and Chambers, A., "Miniature Sensor Probe for O_2, CO_2, and H_2O Monitoring in Portable Life Support Systems," *43rd International Conference on Environmental Systems*, AIAA 2013-3365, Vail, CO, 2013.

[6] Delgado J., Phillips, S., Chullen C., and Mendoza, E., "Compact Multi-gas Monitor for Life Support Systems Control in Space: Evaluation Under Realistic Environmental Conditions," *44th International Conference on Environmental Systems*, ICES 2014-234, Tucson, AZ, 2014.